



IMPERIAL COLLEGE LONDON

DEPARTMENT OF BIOENGINEERING

Submitted in partial fulfilment of the requirements for the award of MEng in  
Biomedical Engineering from Imperial College London

---

Final Report for MEng Project  
**Volumetric Infrared Imaging System for  
the Diagnosis and Monitoring of  
Secondary Lymphoedema**

---

*Author:*

Samuel KARET

*CID:*

01347546

*Supervisor*

Prof James MOORE

Department of Bioengineering

June, 2021

Word Count: 5231

**COVID Statement** The early stages of this project were significantly slowed down due to the COVID-19 pandemic, due to limitations on lab access and the author contracting the virus. The pandemic resulted in delays to the human study, and limits on the number of participants, and also restricted the amount of time that could be spent on testing the device.

## Abstract

The Volumetric Infrared Imaging System (*VIRIS*) developed by the Moore Lab Group at Imperial College London, is a prototype tool for aiding in the diagnosis and monitoring of breast cancer related lymphoedema (*BCRL*).

The objective of this project was to improve the *VIRIS* device, creating a working prototype of suitable size for use in a small consultation room, that can reliably produce volumetric measurements for patients with *BCRL*.

Arm volume of 11 subjects and 1 mannequin arm were measured with both *VIRIS* and by water displacement. Analyses were performed to determine the accuracy of *VIRIS* volume measurements, the accuracy of post-processing with or without Taubin smoothing algorithms, and the most efficient octree depth value for screened Poisson surface reconstruction.

*VIRIS* is capable of taking volume measurements with 2.33% relative error and a coefficient of variation of 1.73% when tested with a mannequin arm, and produces accurate 3D computational models of any scanned appendages. Due to variance in the pose and alignment of human subjects however, the current post-processing methods are not yet robust enough to replicate these results when tested on human subjects ( $n=11$ ), with study results showing a 25% standard deviation from the gold standard of volume measurement.

*VIRIS* is now 50% smaller than its previous iteration, and meets many of the design objectives with respect to size and manoeuvrability, as well as with respect to ease of cleaning, transportation, deployment, and use. Future work is however required, in order to advance the *VIRIS* prototype to comparable levels to alternative volume measurement methods. The use of medial axis transforms and pose transfer methods could be implemented into the post processing to improve the accuracy and reliability with which *VIRIS* obtains volumetric arm measurements, and further design changes could be made to make the prototype more user friendly.

## Acknowledgements

I wish to express my appreciation for all those who helped contribute towards this project. In particular; my supervisor, Prof James Moore Jr, for his advice and feedback; Dr Daniel Watson, for all his help with the software and testing; and Dr Paul Thiruchelvum for his design feedback and input.

# Contents

<b>1</b>	<b>Introduction</b>	<b>3</b>
1.1	Breast Cancer Related Lymphoedema . . . . .	3
1.2	Literature Review . . . . .	3
1.3	Lymphoedema Measuring Methods . . . . .	3
1.3.1	Circumferential Tape Measurement . . . . .	3
1.3.2	Perometry . . . . .	3
1.3.3	LymphaTech . . . . .	4
1.3.4	Biological Impedance . . . . .	4
1.3.5	Water Displacement . . . . .	4
1.3.6	MRI/CT . . . . .	4
1.4	<i>VIRIS</i> . . . . .	4
1.5	Project Aims . . . . .	6

<b>2 Methods</b>	<b>7</b>
2.1 Planning . . . . .	7
2.2 Hardware . . . . .	7
2.2.1 Size Limit Calculations . . . . .	7
2.2.2 Computer Aided Design . . . . .	10
2.2.3 Assembly . . . . .	10
2.3 Software . . . . .	11
2.3.1 Initial Application . . . . .	11
2.3.2 Post-processing Code Collation . . . . .	11
2.3.3 Post-processing Code Method . . . . .	12
2.3.4 Integrated Calibration and Post-processing . . . . .	12
2.3.5 Screened Poisson Surface Reconstruction Analysis . . . . .	12
2.4 Study . . . . .	13
2.4.1 Consent . . . . .	13
2.4.2 Tape Measurements . . . . .	13
2.4.3 Water Displacement . . . . .	13
2.4.4 VIRIS Measurements . . . . .	14
2.5 Validation . . . . .	14
<b>3 Results</b>	<b>15</b>
<b>4 Discussion</b>	<b>20</b>
4.1 Project Evaluation . . . . .	20
4.2 Water Displacement . . . . .	20
4.3 VIRIS . . . . .	20
4.3.1 VIRIS Accuracy . . . . .	20
4.3.2 Validation . . . . .	21
4.3.3 Simulated Swelling Map . . . . .	22
4.4 Future Work . . . . .	22
4.4.1 Improvements to VIRIS . . . . .	22
4.4.2 Further Uses of VIRIS . . . . .	23
<b>5 Conclusion</b>	<b>23</b>
<b>References</b>	<b>24</b>
<b>Appendices</b>	<b>28</b>
<b>A CAD Designs</b>	<b>28</b>
<b>B Bill of Materials</b>	<b>29</b>
<b>C Study Participant Information Document</b>	<b>30</b>
<b>D Study Consent Form</b>	<b>35</b>
<b>E MATLAB Code</b>	<b>36</b>
E.1 Post Processing Testing . . . . .	36

# 1 Introduction <sup>†</sup>

## 1.1 Breast Cancer Related Lymphoedema

Breast cancer related lymphoedema (BCRL) refers to secondary lymphoedema, which presents as swelling of the arm, as a result of breast cancer treatment.<sup>2,3</sup> Breast cancer accounts for 24.5% of new cancer diagnoses in females, with more than 2 million estimated new cases in the year 2020.<sup>4</sup> From the many studies investigating BCRL,<sup>5-12</sup> evidence suggests that 5 year incidence rates could reach as high as 42%,<sup>9</sup> and as many as 1 in 5 recipients of breast cancer treatment experience BCRL within 6 months post-surgery.<sup>7</sup> BCRL can result in a variety of physical (disfigurement, physical discomfort, functional impairment of the arm<sup>8</sup>) and mental (anxiety, depression, emotional distress<sup>13-15</sup>) issues, having a significant impact on quality of life.

## 1.2 Literature Review

A collection of literature regarding lymphoedema and various measuring techniques was analysed, and the strengths and weaknesses of the various methods were identified, as well as possible areas for improvement to take into consideration whilst completing the project.<sup>1</sup>

## 1.3 Lymphoedema Measuring Methods

Secondary lymphoedema is most commonly identified and diagnosed through a variety of methods by which the volume of the arm is measured.<sup>16</sup> Each of these methods has considerations that either increase or decrease their suitability for use depending on the situation.

### 1.3.1 Circumferential Tape Measurement

By using a flexible, non-stretching tape measure, and taking circumferential measurements of the arm at set anatomic points along the extremity.<sup>12</sup> The truncated cone method can then be used with these measurements to calculate the volume of the arm.<sup>17</sup> This is a low cost method, which makes use of a widely available measuring tool and allows for the tracking of localised changes in a lymphoedema; however it simplifies the anatomy by assuming circular circumference, which can result in over or underestimations of the volume. Taking circumferential tape measurements is also a time-consuming process which requires a trained professional, and is prone to variation in measurements depending on the assessor.<sup>17</sup>

### 1.3.2 Perometry

A perometer is a non-invasive optoelectronic device which makes use of two perpendicularly oriented parallel acting light curtains to create elliptical cross-sections of a body part from its shadows and hence quantify its volume.<sup>12</sup> The perometer is mounted to a frame which is moved along the body part to scan it. The perometer has a high precision with a standard deviation of 8.9ml<sup>18</sup> and a large scanning area which allows for easy and hygienic scanning of most body parts. The limiting factor of the perometer is the large size of the device and its high cost. Also, due to the nature of the device taking elliptical cross-sections, it struggles to accurately capture convex areas such as the inner elbow.

---

<sup>†</sup>The following section contains work that has previously been submitted as part of the literature review in the planning report for this project.<sup>1</sup>

### **1.3.3 LymphaTech**

The LymphaTech 3D Imaging System makes use of a commercially available depth camera connected to a smartphone or computer tablet running custom software.<sup>19</sup> The custom software produces a reliable 3-dimensional rendering and volumetric measurement of the arm in real time, with an intraclass correlation coefficient of 0.97, an identical value to that of the perometer.<sup>19</sup> The LymphaTech system is much smaller than a perometer, but requires the camera to be held a certain distance away from the patient,<sup>20</sup> and so is still unsuitable for use within the small consultation rooms typical of breast-cancer clinics. Though it is less time consuming than taking circumferential tape measurements, it takes approximately 40 seconds per arm<sup>19</sup> to scan, and so the entire process takes approximately 4 minutes including positioning of the limb. This requires the patient to hold their arm in position for the entire process of the scan, which could be difficult or painful for patients with severe lymphoedema. Whilst the LymphaTech system is many times cheaper than a perometer (approximately \$1000<sup>20</sup>), there are licensing fees to use the associated software, and experience and training is required to obtain reproducible results.<sup>20</sup>

### **1.3.4 Biological Impedance**

Biological impedance (bioimpedance) measurements are taken by passing electrical currents of varying frequencies through the tissue and calculating the impedance of the tissues between the electrodes.<sup>21</sup> This is a non-invasive procedure and due to the differing electrical properties of intracellular water and extracellular water, the impedance values can be used to determine the volume of extracellular fluid in the tissue.<sup>22</sup> Hence using bioimpedance measurements is effective for early diagnoses of lymphoedema,<sup>2</sup> however access to bioimpedance spectroscopy devices is limited due to their high cost.

### **1.3.5 Water Displacement**

Another method relies on Archimedes' principle of displacement; by submerging the patient's arm in a full open topped container of water, the volume of the submerged limb is equal to the volume of water displaced from the container. Often called the "gold standard" for lymphoedema volume measurement,<sup>17,23,24</sup> this method is considered to be accurate and has a low cost when done properly.<sup>25</sup> However, it does not provide any information about limb shape,<sup>25</sup> is cumbersome and messy,<sup>12,18,25</sup> and there are possible hygiene concerns regarding patients with open wounds.<sup>18</sup>

### **1.3.6 MRI/CT**

Magnetic resonance imaging or computer tomography are also methods which have been used to obtain extracellular fluid volume measurements by determining the cross-sectional composition of a limb across small increments along the length of the limb.<sup>22,25</sup> However, the cost for a single MRI scan in the USA is upwards of \$1000,<sup>26,27</sup> or \$450 in the United Kingdom,<sup>27</sup> with the machines themselves costing \$35,000-\$850,000.<sup>28</sup> A CT scanner has upfront costs upwards of \$350000<sup>29</sup> and a similar figure for yearly maintenance cost.<sup>29</sup> Also, CT uses ionising radiation which is associated with a variety of health issues and so is avoided when other methods are available.

## **1.4 VIRIS**

The Volumetric Infrared Imaging System (VIRIS) is being developed by the Moore Lab Group at Imperial College London as a low cost, fast alternative to current lymphoedema volume measuring methods. It is composed of 3 Intel RealSense D415 depth cameras,<sup>30</sup> arranged in an

equilateral triangle with sides 1.3m in length as shown in the figure below. Its parts include six lengths of 2020 aluminium extrusion, as well as 3D printed corner caps, and six 3D printed calibration orbs, which are attached via brass rods and threaded inserts to 3D printed mounts.<sup>1</sup> The assembly is then mounted to the pneumatic lift of an office chair, with the total cost of parts < £1000. VIRIS is controlled by a MATLAB application that takes 2 sets of 3 simultaneous



Figure 1: Setup of VIRIS at the outset of the project.<sup>†</sup>

point cloud images, the first without the arm, as a calibration image, and the second with the arm, as a scan. Subsequent post processing aligns the point cloud images of the scan using the location of the calibration orbs in the calibration image as reference points.<sup>31</sup> After a series of filters,<sup>31</sup> segmentations, and alignments,<sup>16</sup> the points representing the shoulder are removed,<sup>16</sup> and MeshLab is used to perform a screened Poisson surface reconstruction (Figure 2) of the remaining point clouds to form a mesh which is then further smoothed and saved.<sup>16</sup> The hand is then cut from the mesh, and the open ends of the mesh capped. The volume of the mesh is then calculated, making use of the divergence theorem which links the volume of a mesh to the surface integral across it.<sup>32</sup>

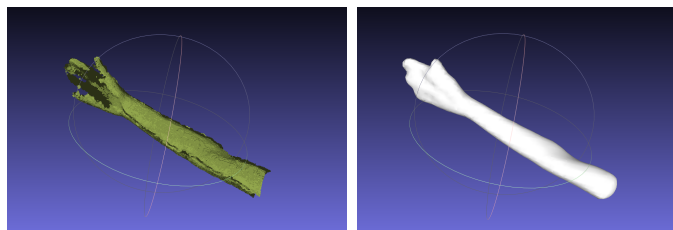


Figure 2: MeshLab renderings before and after screened Poisson surface reconstruction.

VIRIS acquires arm measurements within a few seconds, the majority of which is the user aligning their arm with the device, which is more than twice as fast as the LymphaTech system,<sup>19</sup> and much faster than other methods and requires little to no training.<sup>16</sup> The coefficient of variation for a VIRIS measurement (1.56%)<sup>16</sup> is lower than that of those taken using LymphaTech (1.7%),<sup>33</sup> but it has a large footprint and thus is unsuitable for use in small consultation rooms.

---

<sup>†</sup>Reproduced from Stiansen.<sup>16</sup>

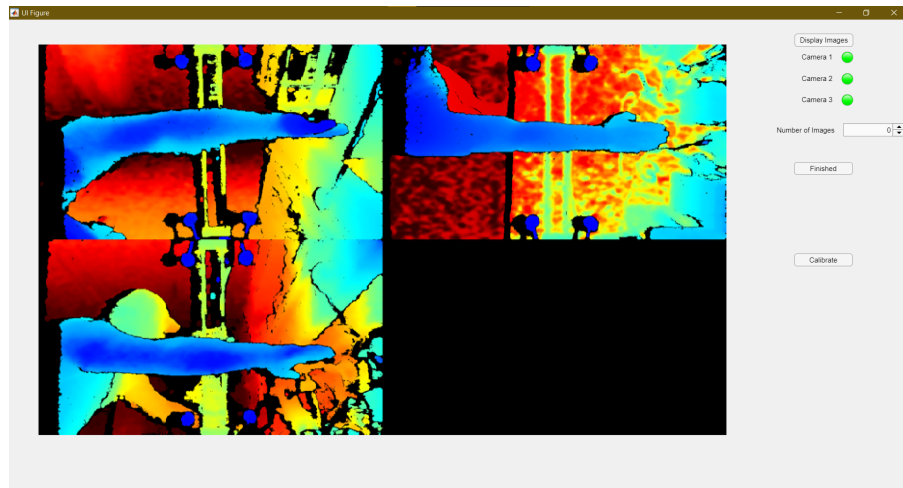


Figure 3: Initial VIRIS MATLAB application GUI.

## 1.5 Project Aims

This project aimed to improve upon the VIRIS apparatus and develop it towards possible clinical use. Discussions with Dr Paul Thiruchelvum, a consultant oncoplastic breast surgeon at Imperial College Healthcare NHS Trust, resulted in a comprehensive list of objectives for the device to meet.<sup>1</sup>

- Reliably producing accurate measurements .
- Having as small a footprint as possible.
- Being easy to manoeuvre about the clinic.
- Being easy to transport between hospitals.
- Being easily cleaned (with antibacterial wipes).
- Being quick to use.
- Being easily deployed.

As such, the foremost goal of this project was to reduce the size of VIRIS so that it would not have any dimensions exceeding 1 metre in length. Secondary goals were to reduce the weight of the device to below 2.5kg, and provide integrated scan processing into the controlling application.

## 2 Methods

### 2.1 Planning

A Gantt chart was produced, containing all the tasks initially considered necessary for the project, and is shown in Figure 4 below. The plan was well adhered to, though complications regarding lab access that arose due to the COVID-19 pandemic somewhat restricted the amount of time that could be spent testing the device.

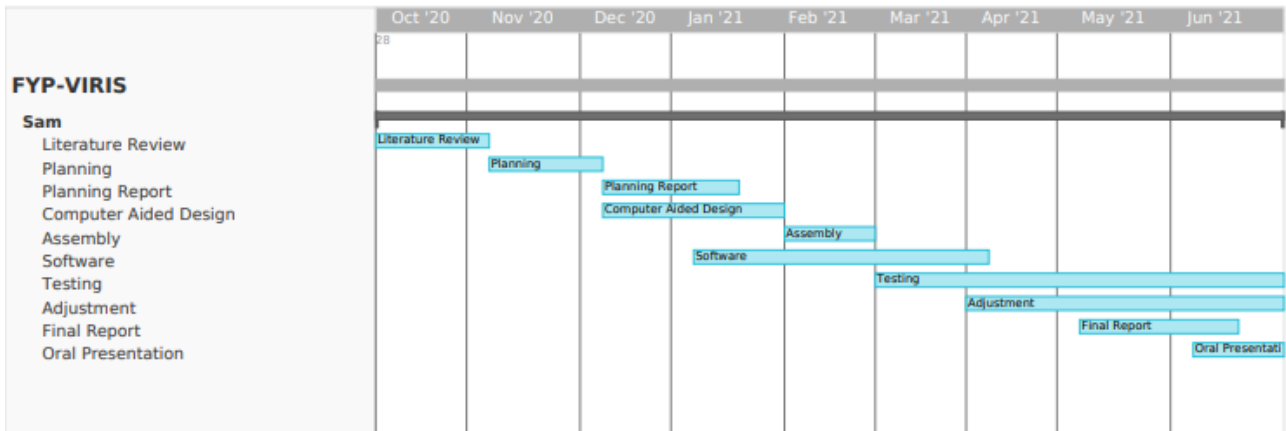


Figure 4: Gantt chart showing planned time frame for the project.

### 2.2 Hardware

#### 2.2.1 Size Limit Calculations<sup>†</sup>

Previous work on the VIRIS project had theorised incorporating a method by which the cameras could be rotated 45° into the device which would allow for a smaller frame size without reducing the maximum arm length that could be measured.<sup>31</sup>

Research into recent improvements in infrared camera technology performance during the literature review showed that some of the more recent releases in the Intel Realsense D400 series have a wider field of view (FOV) than that offered by the D415 module<sup>30</sup> that VIRIS previously used. The Intel RealSense D435 camera was selected as it was the least expensive option to offer the maximum FOV,<sup>30</sup> and then the minimum side length possible for a setup with the newer cameras was calculated.

---

<sup>†</sup>The following section contains work that has previously been submitted as 'Preliminary Work' in the planning report for this project.<sup>1</sup>

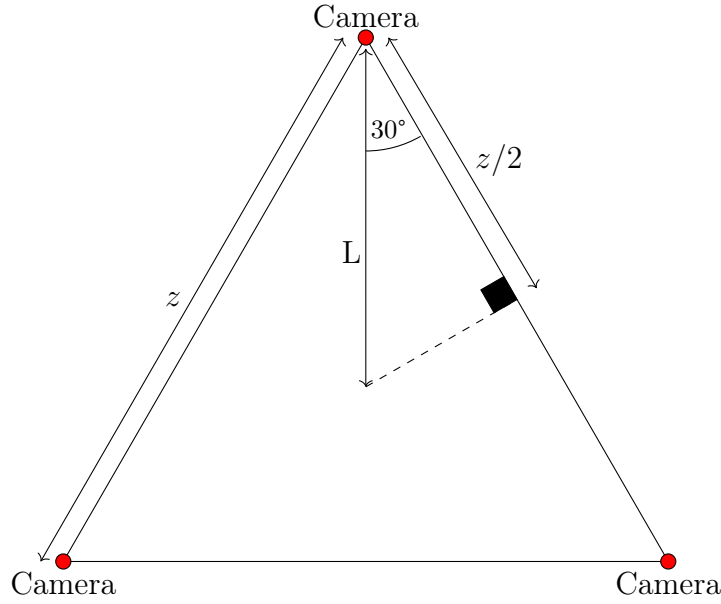


Figure 5: Triangular Representation of the VIRIS Frame - Front View

The newer D435 cameras had an FOV of  $86^\circ$ , whilst the older D415 cameras had an FOV of  $65^\circ$ . From Figure 5, given an equilateral triangle of side length  $z$ ,

$$L = \frac{z}{2\cos(30)} \quad (1)$$

The maximum length of an arm ( $A$ ) that can be measured by a camera attached to a frame with side length  $z$  is therefore:

$$A = 2L \tan\left(\frac{\text{FOV}}{2}\right) \quad (2)$$

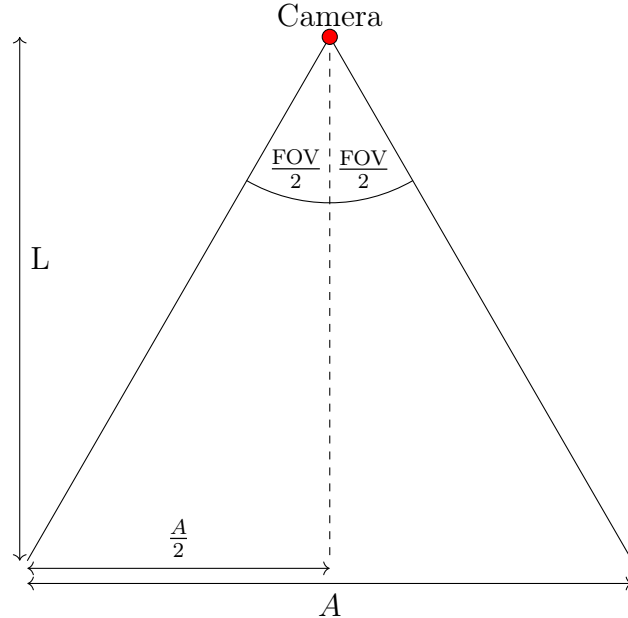


Figure 6: Triangular Representation of the VIRIS Frame - Side View

Hence with the initial setup, using the D415 cameras with  $\text{FOV} = 65^\circ$  and  $z = 1.3m$ , the

maximum length of an arm that could be measured is:

$$A = \frac{z \tan(\frac{\text{FOV}}{2})}{\cos(30)} \quad (3)$$

Which is in this case:

$$A = \frac{1.3 \tan(32.5)}{\cos(30)} = 0.956m \quad (4)$$

This is far longer than a patient's arm is likely to be and thus the device does not need to be so large. Given the length of a human's arm is approximately 40% of their height<sup>34</sup> and assuming that more than 99% of patients are under 2m tall,<sup>35</sup> it can be assumed that  $A = 0.8m$ , therefore the new length of the sides of the frame for the device using D435 cameras would be:

$$z = \frac{A \cos(30)}{\tan(\frac{\text{FOV}}{2})} = \frac{0.8 \cos(30)}{\tan(43)} = 0.743m \quad (5)$$

This would result in a 43% decrease in the length of the sides of the frame, and a 67% decrease in area of the device, significantly reducing its footprint.

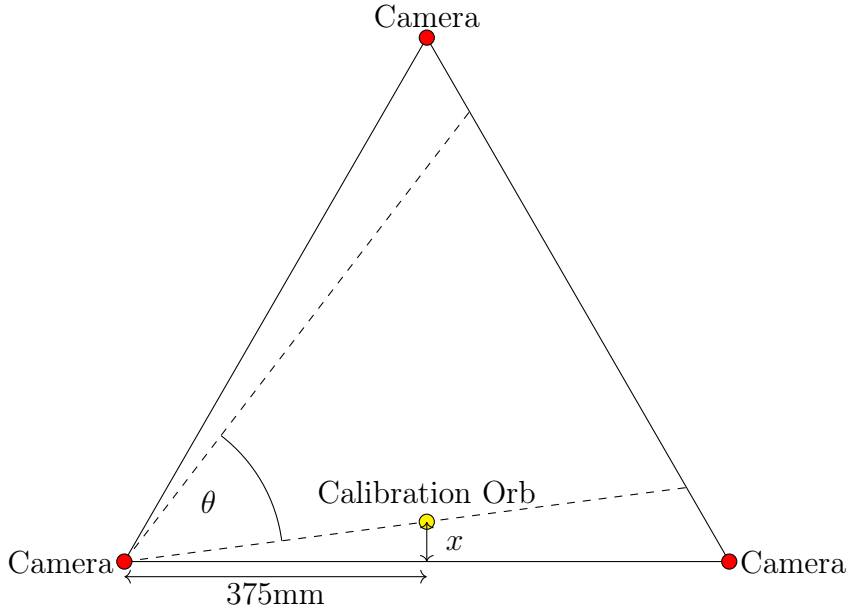


Figure 7: Triangular Representation of the VIRIS Frame - Front View

The calibration orbs of the previous iteration were 60mm in diameter, which was halved for the new version. It was assumed that in order to be seen clearly, the orbs could not sit within the outer 20% of the FOV of the camera. Hence for the angle between the lines drawn from any 2 unpaired calibration orbs to the camera that is positioned between them:

$$\theta < \text{FOV} - 20\% \quad (6)$$

Since the vertical FOV of the D435 cameras is 58°, this allows for any  $\theta$  below 46.4°. Using  $\theta = 45^\circ$ , the angle between any camera's view of its neighbouring orb and the corresponding edge of the device is  $30^\circ - \frac{\theta}{2} = 30^\circ - \frac{45^\circ}{2} = 7.5^\circ$ . Therefore, accounting for the angle at which the mount sits in its bracket, to find the length of the orb mount:

$$L = \frac{375mm \tan 7.5}{\cos 22.5} \approx 55mm \quad (7)$$

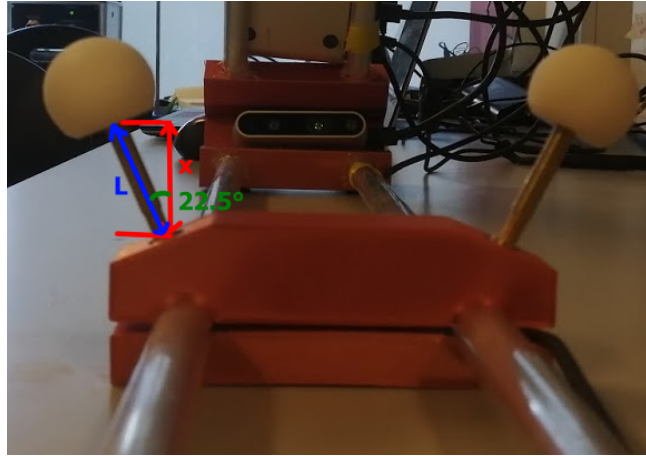


Figure 8: Cross Sectional View of the VIRIS calibration orb mounts.

### 2.2.2 Computer Aided Design

A 3D model of the new design was rendered using Autodesk software, shown below in Figure 9. New calibration orbs with a diameter of 30mm were designed and 3D printed in white 3D printing resin (ANYCUBIC, Shenzhen), and newly designed end caps and calibration orbs were designed and 3D printed in PLA. Iterations of the designs can be found in Appendix A

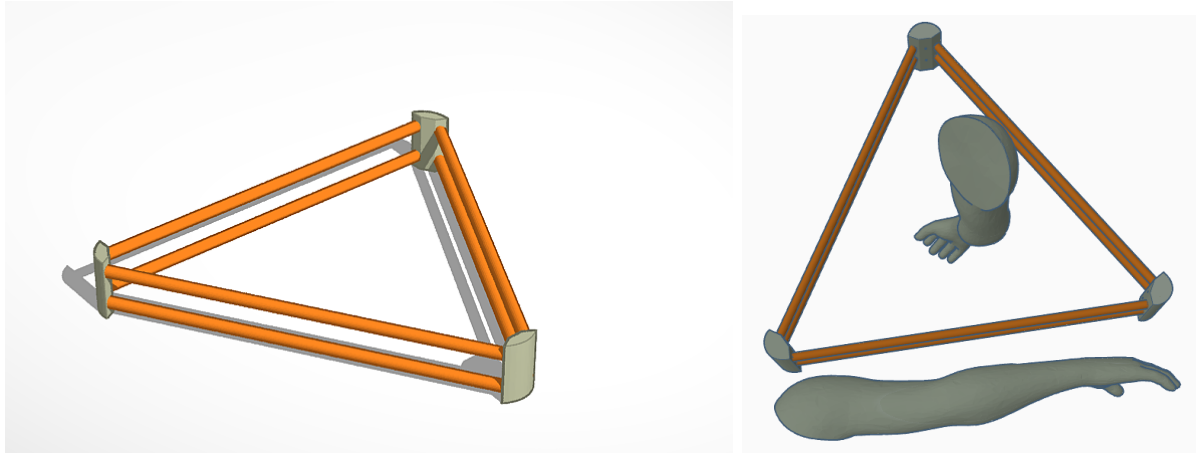


Figure 9: Computer Aided Design renderings of new frame designs

### 2.2.3 Assembly

The end caps were connected by 6 hollow aluminium rods 750mm long with an inner diameter of 12.6mm and an outer diameter of 15.8mm, and hot glued in place. The orbs were mounted onto threaded brass rods 55mm in length which were screwed into threaded inserts in the 3D printed mount brackets, which were themselves clamped halfway along the rods' length with the orbs facing inwards using a single nut and a threaded insert. The cameras were linked to a StarTech TB33A1C by USB Type-A to USB Type-C cables,<sup>36</sup> which were then organised and held down with electrical tape to prevent them from interfering with image capture. The device is then plugged into a 65W DC power supply, and connected by Thunderbolt cable to the controlling PC.



Figure 10: New VIRIS Assembly

## 2.3 Software

The application and associated post-processing code used for this project were all written in MATLAB® r2021a (MathWorks®, Natick) and the built in App Designer. A repository existed from previous iterations of the project, which was updated during the course of this iteration of the project as further work was performed. A link to the repository can be found in Appendix E.

### 2.3.1 Initial Application

An initial application for taking and saving calibration images and scans using the VIRIS device was written, reusing many parts of the code used for the previous iteration of the project.<sup>16</sup> Scans were saved with the identifiers of subject ID number, left or right arm, the scan number, and the time/date at which the scan was taken.

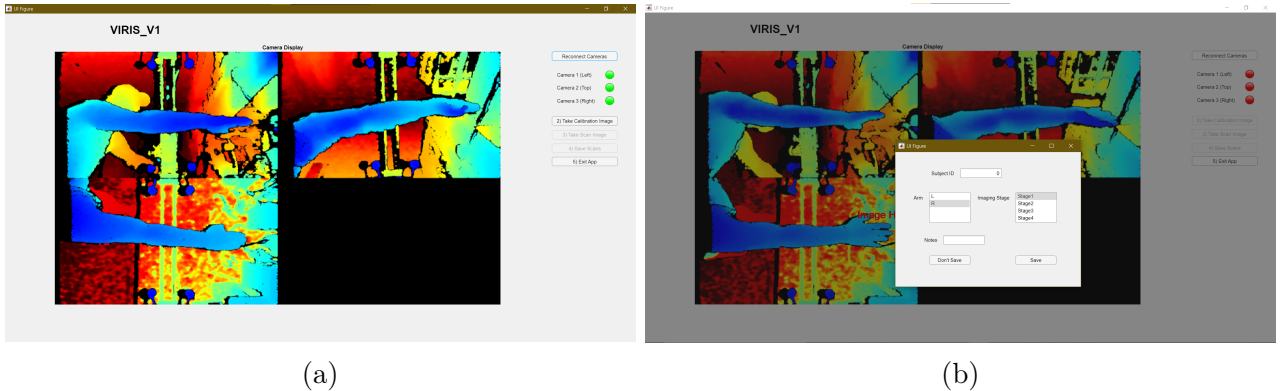


Figure 11: (a) Initial MATLAB application. (b) Save Dialog GUI

### 2.3.2 Post-processing Code Collation

The post-processing code available on the GitHub repository at the start of the current iteration of the project was spread out amongst many files, with parts of different files being required to

perform the methods mentioned by Stiansen.<sup>16</sup> As such, the appropriate code from the various files was collated into an individual working document (of .m file type) and its associated functions, to be used as the basis for further work on the project. Comments were also added to the code for better readability for future work.

### 2.3.3 Post-processing Code Method

First, the saved scan file was loaded, which contained calibration image data, scan data, and 2 variables indicating the measured distances from the fingertip to the ulnar styloid process and shoulder landmark. The calibration image was comprised of 3 point cloud images. The scan data contained 3 point cloud images, as well as the respective texture maps and colour images.

**Calibration** Points outside the expected positions for the calibration orbs were filtered out of the calibration image point clouds; the points were then segmented into clusters by Euclidean distance, and the clusters then sorted by size. The locations of the centers of the 6 largest clusters were calculated, and the rest of the clusters were discarded. The rotation and transformation matrices required to transpose the centers of the calibration orbs in the second and third images over the equivalent in the first image were then calculated, such that the distance between identical balls in separate images was minimised. This was done using a constrained gradient descent method initialised with the cameras at [1,0,0] facing in the [1,0,0] direction. The residual error at the end of the process was then used to establish its success, rejecting any calibration with a total residual error greater than 1cm.

**Meshing** The rotation and transformation matrices were then applied to the pertinent point clouds. The mean of all the points was taken and then subtracted from each point to center the point clouds. The second moment of area was then calculated for each point, with the 6 resulting values undergoing an eigendecomposition to produce a rotation matrix which aligned the point clouds along the axis from fingertip to shoulder. Any points further away from the fingertip than the predefined shoulder landmark were then removed from the point clouds before they were again centered and realigned in the same way as before. The resulting point clouds were saved as temporary .ply files.

The temporary files were input into a script that interacted with MeshLab to apply a series of filters to the point clouds. First, the point clouds were merged with the Flatten Visible Layers filter, and then a screened Poisson surface reconstruction and Taubin smoothing were performed on the merged point cloud. An Invert Faces Orientation filter would be applied to the resulting mesh, before it was saved in .stl form. This was then read back into MATLAB, the hand was cut from the mesh, and the mesh was then recapped to form a closed geometry. The locations of the centroids of all the surface triangles of the mesh, as well as the normal vector and area of the respective triangles were then identified. The sum of the product of these values forming the surface integral of the mesh, which by divergence theorem is equivalent to its volume.<sup>32</sup>

### 2.3.4 Integrated Calibration and Post-processing

A second version of the application was then produced which incorporated the calibration and meshing code as an initial check to prevent calibration or post-processing issues.

### 2.3.5 Screened Poisson Surface Reconstruction Analysis

The method used to transform the 3 point clouds obtained from the D435 cameras into a single mesh was a screened Poisson surface reconstruction, of which a key parameter is the octree

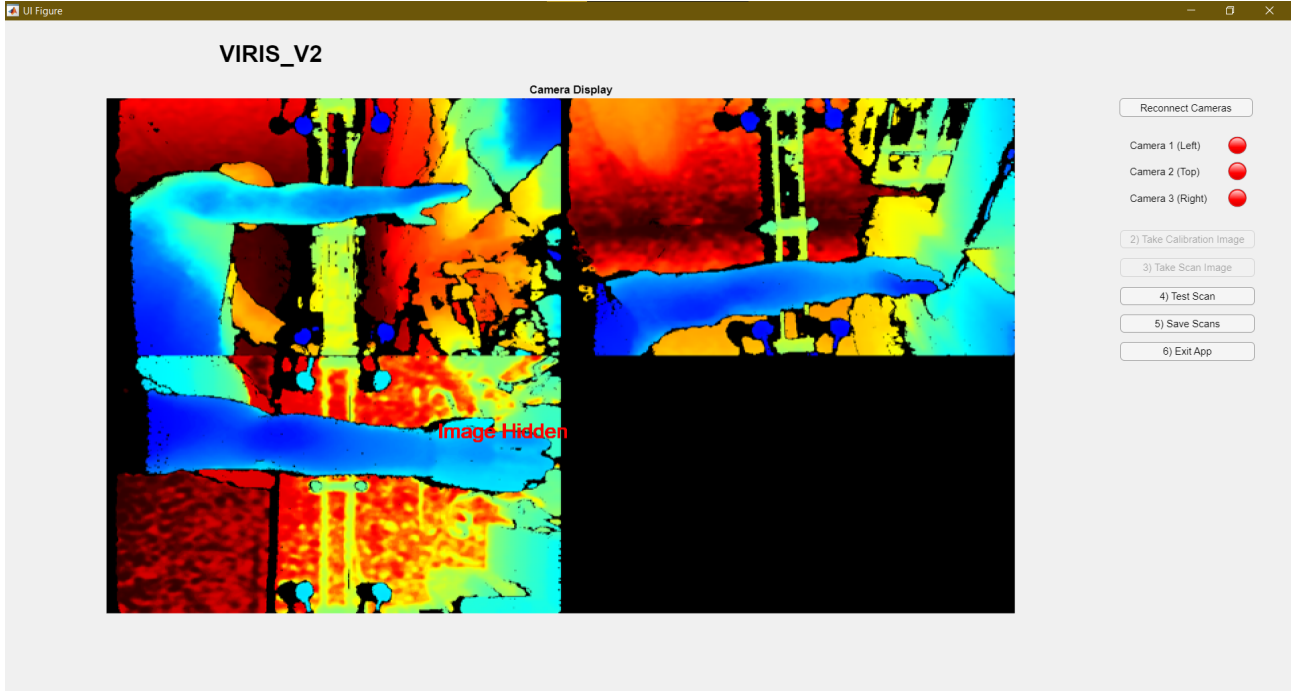


Figure 12: VIRIS MATLAB application GUI with integrated post processing.

depth. As octree depth is increased by 1, the number of nodes contained in the resulting mesh increases by a power of 8, significantly increasing processing times. An analysis of the effect of octree depth on the volume of the mesh produced by the respective screened Poisson surface reconstruction (Figure 21) was performed. 88 scans were processed 6 times, using a screened Poisson surface reconstruction with an octree depth of 2,3,4,5,6, or 10. The maximum octree depth value (which should produce the most accurate mesh) for MeshLab, the software used to perform the screened Poisson surface reconstructions, is 10, and so that was chosen as the basis for comparison.

## 2.4 Study

### 2.4.1 Consent

Ethical approval was obtained from the Imperial College Research Ethics Committee for the study of up to 20 participants, however only 11 participants were studied due to restrictions surrounding the COVID-19 pandemic. The 11 participating subjects were each given a participant information sheet and consent form as shown in Appendices C & D, and the process of the study was also verbally explained to them.

### 2.4.2 Tape Measurements

For each subject, tape measurements of the length from the most distal fingertip to landmarks on the arms were taken and recorded. The landmarks used were the ulnar styloid processes, and a landmark point just below the shoulder.

### 2.4.3 Water Displacement

The water displacement apparatus was setup as shown in Figure 13 above. The tank was emptied and refilled between subjects, and each subject had both of their arms measured using the apparatus once. The process required that the subject first lower their hand into the water



Figure 13: Configuration of the apparatus for the water displacement test.

until the water level was at the center of their ulnar styloid process and the water had settled. Then, the scales would be tared and the subject would lower their arm with their fingers outstretched until their fingertip met a mark on the outside of the tank. This mark varied for the individual subjects and was put at a distance from the water level equal to the distance earlier measured from the subject's fingertip to the upper arm cutoff point. The process for an individual water displacement measurement took approximately 10 minutes, and required 2 minutes to refill between measurements of the same subject, and 12 minutes to replace the water between subjects.

#### 2.4.4 VIRIS Measurements

8 scans were taken of each subject using the VIRIS device. Individual scans were taken of each arm 3 times, and another individual scan was taken of each arm whilst the subject wore a loose compression bandage to simulate a swelling. The controlling application streams data from the cameras, and on a button click, saves the data at that time to a variable. The scan process for an individual scan took <20 seconds, consisting of a calibration image being taken, the arm being aligned with the device, and the scan taken and saved.

### 2.5 Validation

A total of 3 water displacement measurements and 3 VIRIS measurements were taken of a mannequin arm as shown in Figure 18. The relative error of these measurements was calculated as the mean of the absolute difference of each measurement and the mean of the measurements, divided by the mean of the measurements. The coefficient of variation of the measurements was calculated as the standard deviation of the measurements divided by their mean.

### 3 Results

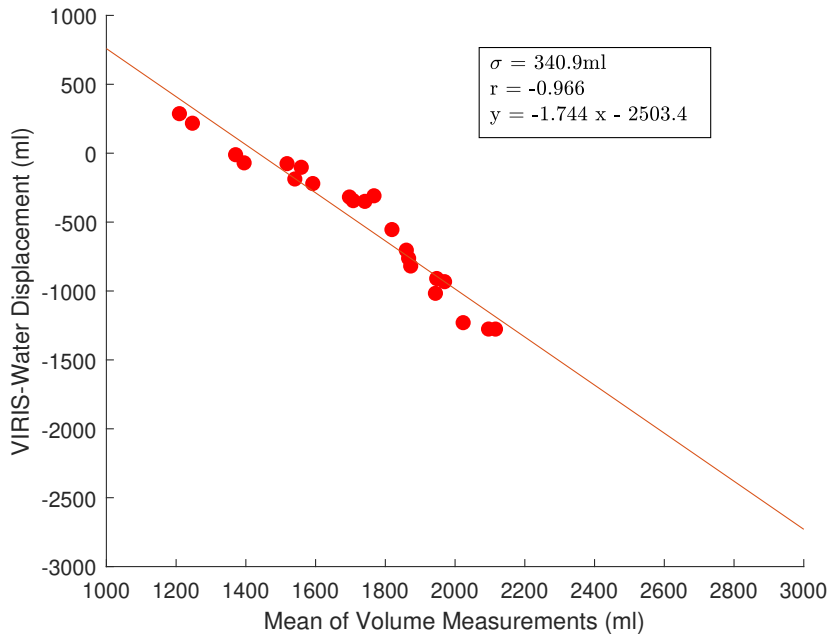


Figure 14: Bland-Altman plot of mean VIRIS volume measurements using the Taubin smooth filter and water displacement volume measurements. The data has a standard deviation of 341ml and a linear regression analysis of it shows strong negative correlation ( $r^2 = 0.93$ ) between the difference between and mean of the measurements of a given limb.

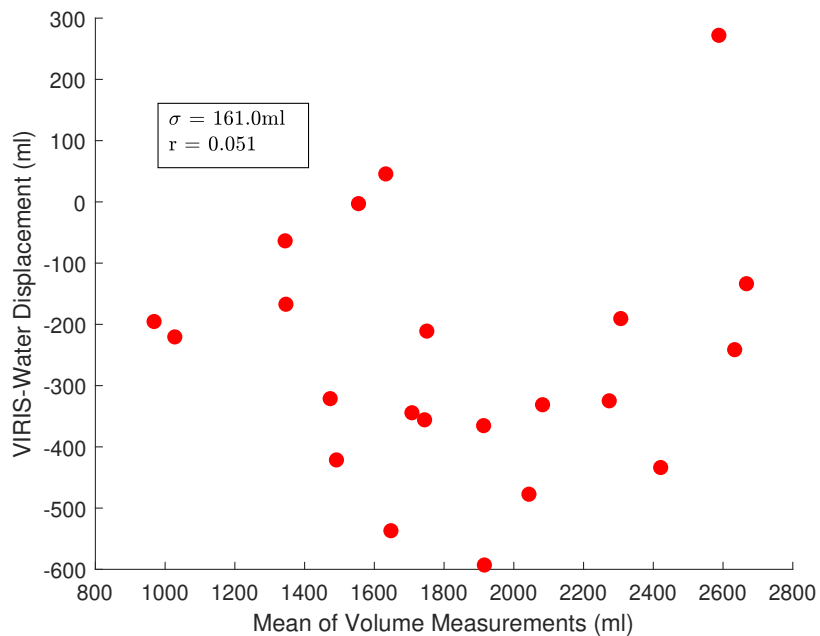


Figure 15: Bland-Altman plot of mean VIRIS volume measurements and water displacement volume measurements without the Taubin smooth. The data has a standard deviation of 161ml and a linear regression analysis of it shows no correlation ( $r^2 = 0.0026$ ) between the difference between and mean of the measurements of a given limb.

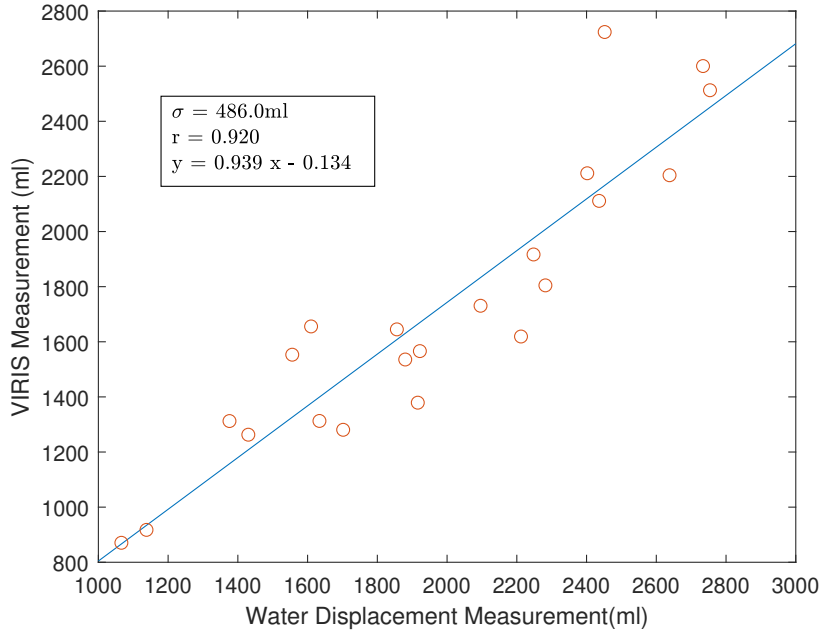


Figure 16: Plot of VIRIS measurements against corresponding water displacement measurements. The data has a standard deviation of 486ml and a linear regression analysis of it shows strong positive correlation ( $r^2 = 0.85$ ) between VIRIS measurements and water displacement measurements of a given limb .

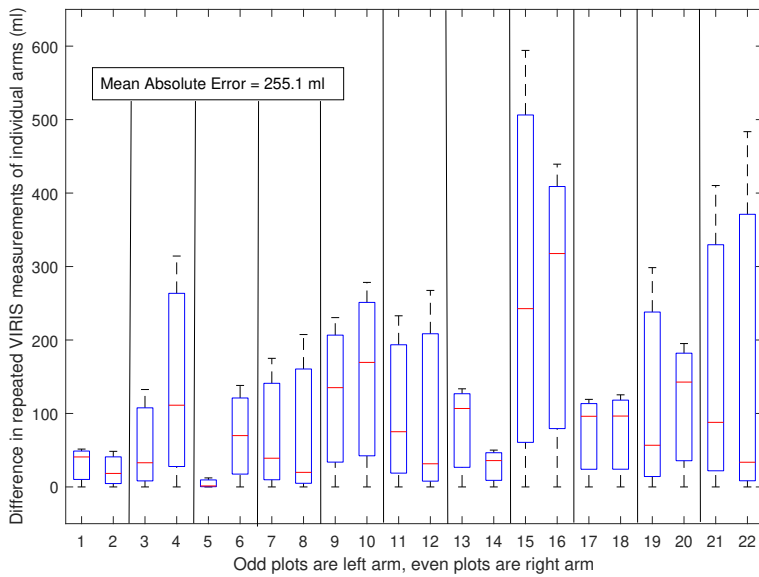


Figure 17: Box and whisker plot showing difference in VIRIS measurements. Mean absolute error was 255ml. Some subjects had much more accurate VIRIS measurements (Range=50ml) than others (Range=594ml).

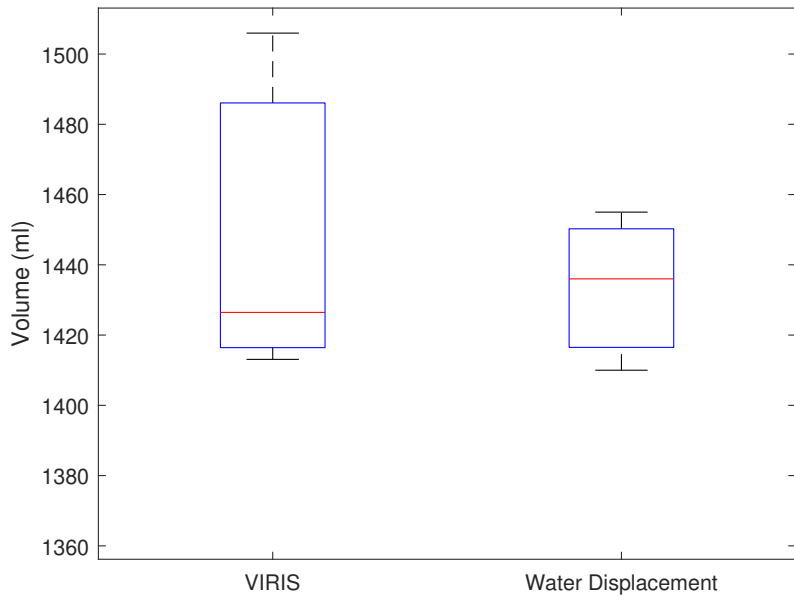


Figure 18: Boxplot of volume measurements taken of a mannequin arm with VIRIS and water displacement. Coefficient of variation for VIRIS is 1.73%. Coefficient of variation for water displacement is 1.29%. VIRIS relative error using water displacement as ‘gold standard’<sup>17,23,24</sup> is 2.33% in comparison to 1.1% for water displacement.

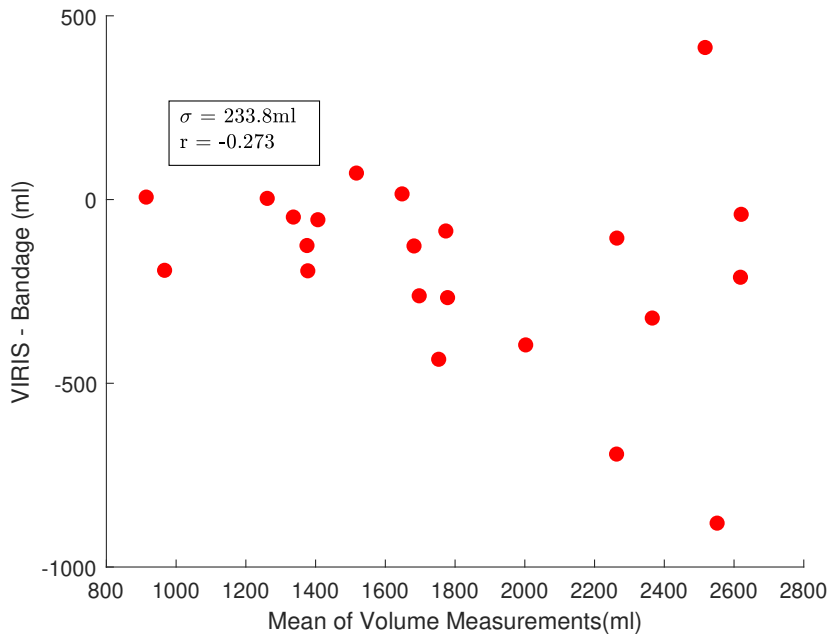


Figure 19: Bland-Altman plot of VIRIS measurements with and without a bandage to simulate lymphoedema. The data has a standard deviation of 234ml and a linear regression analysis of it shows very little correlation ( $r^2 = 0.075$ ) between the size of the limb and the difference in volume measurement caused by the simulated swelling.

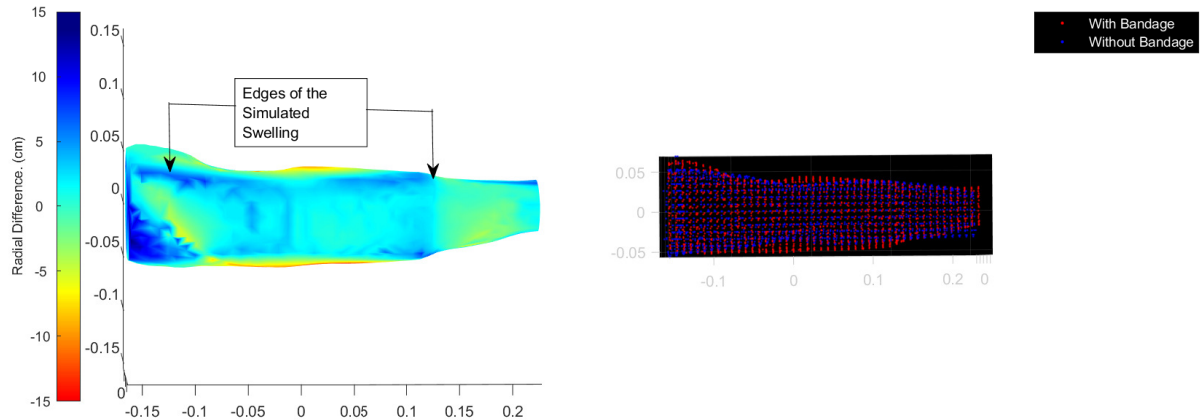


Figure 20: Swelling map showing the radial difference between an arm with a compression bandage to simulate a swelling and the same arm without said bandage (Left), and the co-registered point clouds used to produce the swelling map (Right).

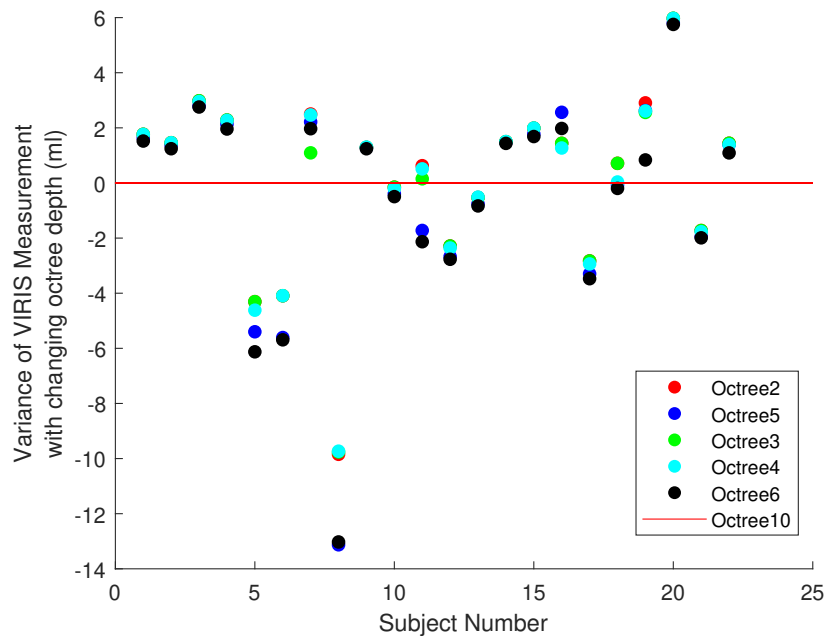


Figure 21: Scatter plot showing how VIRIS volume measurement differs with octree depth value for screened Poisson surface reconstruction compared to the measurements from the most detailed meshes produced with an octree depth value of 10.

Octree Depth	Processing Time(s)
2	356
3	355
4	358
5	278
6	436
7	823
10	3482

Table 1: Table showing processing times for code using varying octree depth values for performing a screened Poisson surface reconstruction. All 88 scans from the study were sequentially post-processed (Appendix E.1), with the processing times quoted being how long it took for all 88 scans to be processed.

Reducing the octree depth to 2, whilst resulting in a mesh with 512 times fewer nodes, made little difference to processing time, though increasing it to 10 resulted in processing times 15 times longer, and meshes with 32768 times more nodes (Table 1). Figure 21 shows that the difference between the volumes of meshes produced using differing octree depth values and that of those produced with an octree depth value of 10 was never  $>14\text{ml}$ , and in the majority of cases, was  $<4\text{ml}$ , which is less than 0.4% the volume of the smallest arms measured in the study. As such, an octree depth of 5 should be used for any post processing integrated into the operating system for VIRIS, as it is the optimal value for increasing number of nodes in the resulting mesh before processing time significantly increases.

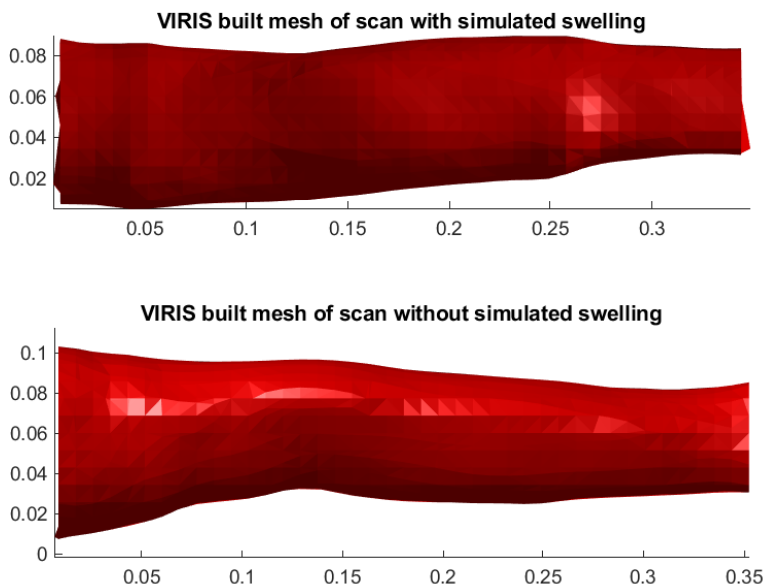


Figure 22: Examples of the final mesh of which VIRIS calculates the volume.

## 4 Discussion

### 4.1 Project Evaluation

Using the objectives outlined in Section 1.5 as a basis for evaluation, at the conclusion of the allocated time for working on the project, many of the limitations of VIRIS identified at the outset of the project have been overcome, whilst others still require further work to meet the required specification for clinical use. The VIRIS apparatus has been reduced to 50% of its previous footprint, making it suitable for use in much smaller rooms than the previous iteration. It is also much more lightweight (2.134kg) and easily transported than previously. The entire device can be easily cleaned with antiseptic wipes, is quick to use, and is easily deployed. The total cost of all the parts to produce the VIRIS assembly is less than £700 and a full bill of materials can be found in Appendix B. Further work is required however, to ensure that VIRIS reliably produces accurate measurements, and several ideas as to how this can be achieved are outlined in Section 4.4.

### 4.2 Water Displacement

The volumeter used for the water displacement measurements, shown in Figure 13, was unwieldy and uncomfortable to use, due to its excessive size. It was constructed of 9mm thick clear acrylic plastic, with a square base 260mm\*260mm, and sides 1260mm tall. A half pipe with diameter 25mm was positioned aligned with the top of the structure and the structure was glued together with aquarium cement. This setup resulted in some participants having to stand on a step-ladder in order to take the measurement. A noticeable amount of water also appeared to overflow as a result of the water surface oscillating due to arm movement. This could have been mitigated using a different volumeter setup, of which there are a variety,<sup>17,37,38</sup> with some being especially resistant to rapid oscillations.<sup>38</sup>

### 4.3 VIRIS

The VIRIS apparatus is quick and easy to set up, the process taking less than a minute and only entailing connecting one plug to mains power, connecting a thunderbolt cable to the controlling PC, and running the MATLAB application. VIRIS weighs only 2.134kg, which whilst heavier than the Lymphatech system,<sup>19</sup> is far lighter than perimeters, MRI machines, or water displacement setups. It is also small enough that it is capable of taking measurements in any space large enough for the patient to fully extend their arm.

For the study, the apparatus was positioned on a tabletop, and most participants quickly got used to its usage, either crouching, or sitting on a chair in order to align their arm with the center of the device. At the time of the study, though the checks built in to the software to ensure the viability of the calibration images worked as intended, the post-processing code at the time was error-prone. These errors often resulted in the app becoming non-responsive, which required MATLAB to be restarted, a process which took approximately 2 minutes each time.

#### 4.3.1 VIRIS Accuracy

**Study Measurements** Figure 14 shows that the volume measurements taken using VIRIS had a clear systematic error of which more than 90% ( $r^2 = 0.93$ ) could be considered to be correlated to the volume of the measured arm. This systematic error was hypothesised to be caused by the Taubin smoothing algorithm, and so the scans were reprocessed using only a screened Poisson surface reconstruction and face orientation inversion. A Bland-Altman

plot (Figure 15) of the reprocessed data was produced, and the regression analysis performed on it indicated that the remaining error in the VIRIS measurements is not correlated to the volume of the arm being measured ( $r^2 = 0.0021$ ). Whilst the VIRIS volume measurements taken for the arms of the study participants were strongly correlated to the corresponding water displacement measurements (Figure 16  $r^2 = 0.85$ ), they showed a much greater variation in results (Figure 17), with a mean absolute error of 255ml. Though Figure 17 also shows that VIRIS measurements for certain subjects were far more accurate than for others, with measurements for 37% of subjects varying by less than 150ml, whilst others varied by more than 300ml.

**Limitations** The author suspects that the cause of the remaining error stems from the post processing software incorrectly measuring the length along the arm at which the boundaries of the volumetric measurement should be taken. Currently, the point clouds are aligned along the x-axis, and then all points with an x coordinate above the distance measured to the shoulder landmark are removed. The remaining point clouds are then re-aligned with the x-axis, and all the points with an x coordinate below the distance measured to the ulnar styloid process are removed from the point cloud. Since the arm is rarely perfectly straight, cutting across a fixed length in space results in the cuts deviating from the predetermined position, and hence a mesh which represents a larger proportion of the arm than otherwise intended. This is shown in Figure 23 where the length of the arm represented by the mesh should be 33cm, however, the volume within the boxed area is in excess of what should be measured, as the axis the mesh is aligned along is not medial to the arm.

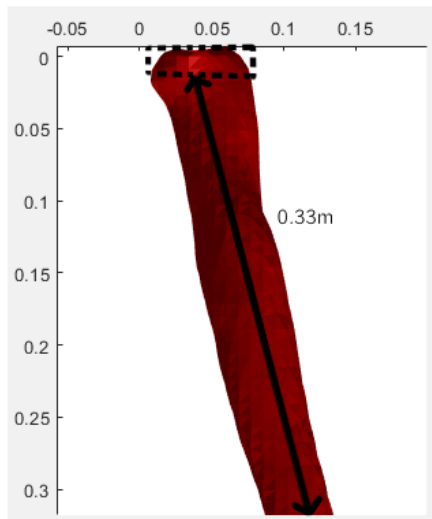


Figure 23: Example of mesh size error due to cutting at a fixed length in space.

#### 4.3.2 Validation

The measurements of the mannequin arm as shown in Figure 18 produced a relative error of 2.33% for the VIRIS measurements compared to the water displacement measurements. The relative error for the water displacement measurements was less than half of that at 1.1%, providing further justification for its use as the ‘gold standard’ for volume measurement.<sup>17, 23, 24</sup> The overall coefficient of variation was 1.73%, similar to that of the LymphaTech device.<sup>33</sup> This indicates that VIRIS is capable of producing accurate volumetric measurements, though the results from the study would suggest further work is required to improve the reliability with which it does.

### 4.3.3 Simulated Swelling Map

Figure 19 shows there is not enough correlation ( $r^2 = 0.075$ ) between the size of the arm and the difference between the pre-post swelling simulation to justify using a compression bandage to reliably produce a predictable change in volume for an arm of given length. Figure 20 however, shows that the swelling maps produced by simulating swelling using compression bandages can still show radial differences, much the same as it would in an arm pre-post lymphoedema.

## 4.4 Future Work

### 4.4.1 Improvements to VIRIS

VIRIS is currently a prototype, and as such there are many improvements that could be made to the apparatus before a version is created that could be widely used as a diagnostic tool.

**Hardware** Currently VIRIS lies flat on the base of the triangular measuring area, so it is the burden of the user to align their arm with the device. Future iterations may include methods to adjust the height of the device. Previous iterations of the device were mounted to the hydraulic base of an office chair, though this itself had issues as large forces were required to lower the system. A system using lead screws and stepper motors to raise and lower the device has been discussed, but not yet designed.

The current cable management system on VIRIS is electrical tape holding the cables to the structure, and whilst the system is still easily cleaned and the cables don't tend to tangle, future iterations should look at other cable management methods such as trunking to prevent cables snagging on objects during transport.

Currently, the assembly is held together by hot glue, and as such requires some care when handled. Future work could replace the 3D printed parts with aluminium milled parts, which would increase the weight of the device, but the parts could then be welded together for a much more sturdy device. Alternatively, changes could be made to the design of the 3D printed end caps and a stronger glue such as two part epoxy could be used to better adhere the plastic parts to the metal rods.

**Graphical User Interface** Much of the MATLAB application is controlled through processes in a single loop, which often results in the entire application crashing when one part of it fails. Future versions of the application should decentralise the control system for taking and saving calibration and scan images. There are a variety of small bugs and user interface glitches that need to be fixed in future versions, such as the application's tendency to throw an error after closing, and the save confirmation message appearing regardless of save state. The current save dialog also limits indexing of files to a maximum of 4 scans per arm per patient, and future iterations could remove that limit. The save dialog could also be edited to automatically number the scan for more consistent file indexing.

The application is currently programmed in MATLAB, an interpreted programming language, which thus takes more time to execute code. Future work could rebuild the application in a compiled programming language, likely C++ or Python, as interpreting the D435 cameras relies on the librealsense SDK, which also has wrappers in those languages.

**Post Processing** As much of the error in VIRIS measurements is currently attributed to cutting in the wrong place when cutting the mesh at the ulnar styloid process and shoulder landmarks, further work could look at methods to better assess the location of the landmarks. The current method is to align the arms as best as possible along the x-axis and then cut the yz-plane of the mesh at a given distance along the x-axis from the fingertip. Another method

to be considered that might produce better results is performing a medial axis transform to locate the medial axis of the mesh, and cutting the mesh normal to the medial axis at a given distance along the medial axis from the fingertip.

#### 4.4.2 Further Uses of VIRIS

As VIRIS produces a 3-dimensional mesh of the patient's arm, volume measurements are not the only data that can be obtained. Further work could use VIRIS to take circumferential measurements of the arm at given landmarks, to be compared to circumferential tape measurements taken by a professional nurse. It could also be used to compare volume measurements obtained using the truncated cone approximation with differing numbers of circumferential measurements to identify the most efficient number of tape measurements required in a clinical setting.

VIRIS could use the obtained point cloud data to identify changes in swelling maps between scans of the same arm, which might possibly be achieved through the use of coupled quasi-harmonic bases<sup>39</sup> in the post processing stage. Pose transfer methods that employ coupled quasi-harmonic bases are more accurate than current non-rigid coregistration methods,<sup>40,41</sup> and could also be used to computationally straighten scans of arms to help avoid alignment errors.

## 5 Conclusion

VIRIS is a promising diagnostic tool for BCRL and has been reduced to a suitable size for use in clinical settings, but requires further improvements to its post processing code before it can reliably provide accurate volumetric measurements.

## References

- [1] S. Karet, “VIRIS - Final Year Project Planning Report,” tech. rep., Imperial College London, Jan. 2021.
- [2] B. J. Smoot, J. F. Wong, and M. J. Dodd, “Comparison of Diagnostic Accuracy of Clinical Measures of Breast Cancer–Related Lymphedema: Area Under the Curve,” *Archives of Physical Medicine and Rehabilitation*, vol. 92, pp. 603–610, Apr. 2011. Publisher: Elsevier.
- [3] P. S. Mortimer, “The pathophysiology of lymphedema,” *Cancer*, vol. 83, no. S12B, pp. 2798–2802, 1998.
- [4] “Globocan 2020 Breast Cancer Factsheet.” <https://gco.iarc.fr/today/data/factsheets/cancers/20-Breast-fact-sheet.pdf>. Online; Accessed 31-12-2020.
- [5] A. C. P. Ribeiro Pereira, R. J. Koifman, and A. Bergmann, “Incidence and risk factors of lymphedema after breast cancer treatment: 10 years of follow-up,” *The Breast*, vol. 36, pp. 67–73, Dec. 2017.
- [6] S. C. Hayes, S. Rye, D. Battistutta, and B. Newman, “Prevalence of Upper-Body Symptoms Following Breast Cancer and Its Relationship with Upper-Body Function and Lymphedema,” *Lymphology*, vol. 43, pp. 178–187, Aug. 2010. Number: 4.
- [7] S. C. Hayes, K. Johansson, N. L. Stout, R. Prosnitz, J. M. Armer, S. Gabram, and K. H. Schmitz, “Upper-body morbidity after breast cancer,” *Cancer*, vol. 118, no. S8, pp. 2237–2249, 2012.
- [8] S. Michael, S. Charikleia, and K. Konstantinos, “Lymphedema and breast cancer: a review of the literature,” *Breast Cancer*, vol. 18, pp. 174–180, July 2011.
- [9] S. A. Norman, A. R. Localio, S. L. Potashnik, H. A. Simoes Torpey, M. J. Kallan, A. L. Weber, L. T. Miller, A. DeMichele, and L. J. Solin, “Lymphedema in Breast Cancer Survivors: Incidence, Degree, Time Course, Treatment, and Symptoms,” *Journal of Clinical Oncology*, vol. 27, pp. 390–397, Jan. 2009.
- [10] J. M. Binkley, S. R. Harris, P. K. Levangie, M. Pearl, J. Guglielmino, V. Kraus, and D. Rowden, “Patient perspectives on breast cancer treatment side effects and the prospective surveillance model for physical rehabilitation for women with breast cancer,” *Cancer*, vol. 118, no. S8, pp. 2207–2216, 2012.
- [11] N. L. S. Gergich, L. A. Pfalzer, C. McGarvey, B. Springer, L. H. Gerber, and P. Soballe, “Preoperative assessment enables the early diagnosis and successful treatment of lymphedema,” *Cancer*, vol. 112, no. 12, pp. 2809–2819, 2008.
- [12] S. F. Shaitelman, K. D. Cromwell, J. C. Rasmussen, N. L. Stout, J. M. Armer, B. B. Lasinski, and J. N. Cormier, “Recent Progress in Cancer-Related Lymphedema Treatment and Prevention,” *CA: a cancer journal for clinicians*, vol. 65, no. 1, pp. 55–81, 2015.
- [13] M. J. Brennan and L. T. Miller, “Overview of treatment options and review of the current role and use of compression garments, intermittent pumps, and exercise in the management of lymphedema,” *Cancer*, vol. 83, pp. 2821–2827, Dec. 1998.

- [14] C. M. A. Badger, J. L. Peacock, and P. S. Mortimer, “A randomized, controlled, parallel-group clinical trial comparing multilayer bandaging followed by hosiery versus hosiery alone in the treatment of patients with lymphedema of the limb,” *Cancer*, vol. 88, no. 12, pp. 2832–2837, 2000.
- [15] A. Szuba, R. Achalu, and S. G. Rockson, “Decongestive lymphatic therapy for patients with breast carcinoma-associated lymphedema,” *Cancer*, vol. 95, no. 11, pp. 2260–2267, 2002.
- [16] N. Stiansen, “MRes thesis,” tech. rep., Imperial College London, 2018.
- [17] T. Deltombe, J. Jamart, S. Recloux, C. Legrand, N. Vandenbroucke, S. Theys, and P. Hanson, “Reliability and Limits of Agreement of Circumferential, Water Displacement, and Optoelectronic Volumetry in the Measurement of Upper Limb Lymphedema,” *Lymphology*, vol. 40, pp. 26–34, Aug. 2007. Number: 1.
- [18] S. Tierney, M. Aslam, K. Rennie, and P. Grace, “Infrared optoelectronic volumetry, the ideal way to measure limb volume,” *European Journal of Vascular and Endovascular Surgery: The Official Journal of the European Society for Vascular Surgery*, vol. 12, pp. 412–417, Nov. 1996.
- [19] J. M. Binkley, M. J. Weiler, N. Frank, L. Bober, J. B. Dixon, and P. W. Stratford, “Assessing Arm Volume in People During and After Treatment for Breast Cancer: Reliability and Convergent Validity of the LymphaTech System,” *Physical Therapy*, vol. 100, pp. 457–467, Mar. 2020. Publisher: Oxford Academic.
- [20] C. Zhou, C. Yahathugoda, L. D. Silva, U. Rathnayaka, G. Owen, M. Weerasooriya, R. U. Rao, G. J. Weil, and P. J. Budge, “Portable infrared imaging for longitudinal limb volume monitoring in patients with lymphatic filariasis,” *PLOS Neglected Tropical Diseases*, vol. 13, p. e0007762, Oct. 2019. Publisher: Public Library of Science.
- [21] B. H. Cornish, I. H. Bunce, L. C. Ward, L. C. Jones, and B. J. Thomas, “Bioelectrical impedance for monitoring the efficacy of lymphoedema treatment programmes,” *Breast Cancer Research and Treatment*, vol. 38, pp. 169–176, June 1996.
- [22] B. H. Cornish, M. Chapman, C. Hirst, B. Mirolo, I. H. Bunce, L. C. Ward, and B. J. Thomas, “Early Diagnosis of Lymphedema Using Multiple Frequency Bioimpedance,” *Lymphology*, vol. 34, pp. 2–11, Aug. 2001. Number: 1.
- [23] J. T. Hidding, P. B. Viehoff, C. H. Beurskens, H. W. van Laarhoven, M. W. Nijhuis-van der Sanden, and P. J. van der Wees, “Measurement Properties of Instruments for Measuring of Lymphedema: Systematic Review,” *Physical Therapy*, vol. 96, pp. 1965–1981, Dec. 2016.
- [24] A. R. Sharkey, S. W. King, R. Y. Kuo, S. B. Bickerton, A. J. Ramsden, and D. Furniss, “Measuring Limb Volume: Accuracy and Reliability of Tape Measurement Versus Perometer Measurement,” *Lymphatic Research and Biology*, vol. 16, pp. 182–186, Sept. 2017. Publisher: Mary Ann Liebert, Inc., publishers.
- [25] A. W. B. Stanton, C. Badger, and J. Sitzia, “Non-Invasive Assessment of the Lymphedematous Limb,” *Lymphology*, vol. 33, pp. 122–135, Aug. 2000. Number: 3.
- [26] S.-j. Wu, G. Sylwestrzak, C. Shah, and A. DeVries, “Price Transparency For MRIs Increased Use Of Less Costly Providers And Triggered Provider Competition,” *Health Affairs*, vol. 33, pp. 1391–1398, Aug. 2014. Publisher: Health Affairs.

- [27] “Average price MRI in selected countries 2017.”  
<https://www.statista.com/statistics/312020/price-of-mri-diagnostics-by-country/>. Online; Accessed 2021-01-11.
- [28] “How Much Does an MRI Machine Cost? - LBN MedicalLBN Medical.”  
<https://lbnmedical.com/how-much-does-an-mri-machine-cost/>. Online; Accessed 2021-06-13.
- [29] H. Abrams and B. Mcneil, “Computed tomography: Cost and efficacy implications,” *AJR. American journal of roentgenology*, vol. 131, pp. 81–7, Aug. 1978.
- [30] “Intel-RealSense-D400-Series-Datasheet-June-2020.pdf.”  
<https://www.intelrealsense.com/wp-content/uploads/2020/06/Intel-RealSense-D400-Series-Datasheet-June-2020.pdf>. Online; Accessed 2020-10-22.
- [31] M. Nasr, “MEng Thesis,” tech. rep., Imperial College London, 2020.
- [32] K. Karakashian, L. Shaban, C. Pike, and R. van Loon, “Investigation of Shape with Patients Suffering from Unilateral Lymphoedema,” *Annals of Biomedical Engineering*, vol. 46, pp. 108–121, Jan. 2018.
- [33] C. Yahathugoda, M. J. Weiler, R. Rao, L. D. Silva, J. B. Dixon, M. V. Weerasooriya, G. J. Weil, and P. J. Budge, “Use of a Novel Portable Three-Dimensional Imaging System to Measure Limb Volume and Circumference in Patients with Filarial Lymphedema,” *The American Journal of Tropical Medicine and Hygiene*, vol. 97, pp. 1836–1842, Dec. 2017. Publisher: The American Society of Tropical Medicine and Hygiene.
- [34] “Anthropometric Data Sheet.”  
[https://bb.imperial.ac.uk/bbcswebdav/pid-1644433-dt-content-rid-5699880\\_1/courses/EH201910/EH201910%20Formula%20sheet%202019-20\\_v2.pdf](https://bb.imperial.ac.uk/bbcswebdav/pid-1644433-dt-content-rid-5699880_1/courses/EH201910/EH201910%20Formula%20sheet%202019-20_v2.pdf). Online; Accessed 2021-01-03.
- [35] “Cumulative Percent Distribution of Population by Height and Sex,” *U.S Census Bureau, Statistical Abstract of the United States*, p. 1, 2011.
- [36] “StarTech TB33A1C Data Sheet.”  
<https://www.bechtle.com/shop/medias/5c77b77c9ce969197d0499a1.pdf>? Online; Accessed 2021-06-13.
- [37] M. Hameeteman, A. C. Verhulst, R. D. Vreeken, T. J. J. Maal, and D. J. O. Ulrich, “3D stereophotogrammetry in upper-extremity lymphedema: An accurate diagnostic method,” *Journal of Plastic, Reconstructive & Aesthetic Surgery*, vol. 69, pp. 241–247, Feb. 2016.
- [38] L. W. Weiss, T. R. Ireland, A. A. Friedman, A. C. Fry, and Y. Li, “Functional Submersion Technique for Assessing Volume,” *Measurement in Physical Education and Exercise Science*, vol. 4, pp. 199–213, Dec. 2000. Publisher: Routledge.
- [39] A. Kovnatsky, M. M. Bronstein, A. M. Bronstein, K. Glashoff, and R. Kimmel, “Coupled quasi-harmonic bases,” *arXiv:1210.0026 [cs]*, Sept. 2012. arXiv: 1210.0026.
- [40] M. Yin, G. Li, H. Lu, Y. Ouyang, Z. Zhang, and C. Xian, “Spectral pose transfer,” *Computer Aided Geometric Design*, vol. 35-36, pp. 82–94, May 2015.

- [41] S. C. Schonsheck, M. M. Bronstein, and R. Lai, “Nonisometric Surface Registration via Conformal Laplace–Beltrami Basis Pursuit,” *Journal of Scientific Computing*, vol. 86, p. 30, Mar. 2021.

# Appendices

## A CAD Designs

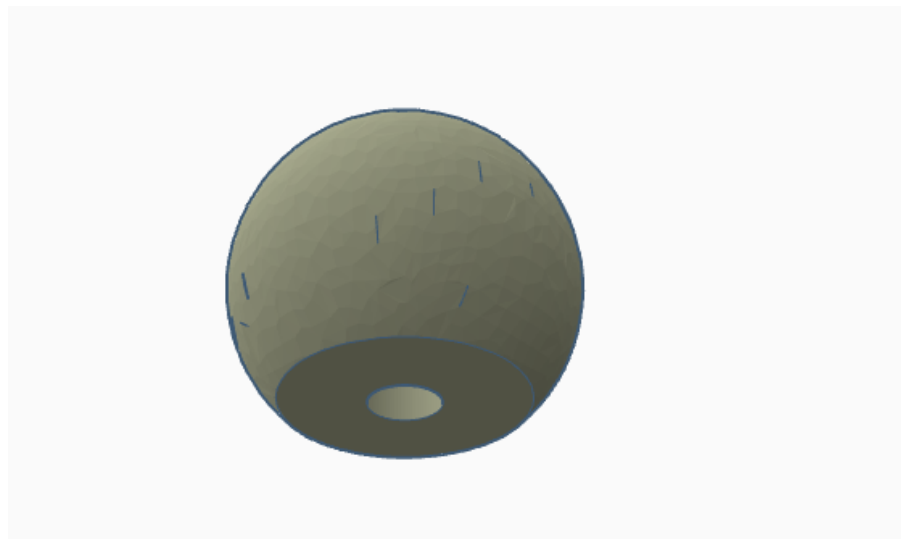


Figure 24: Calibration Orb CAD

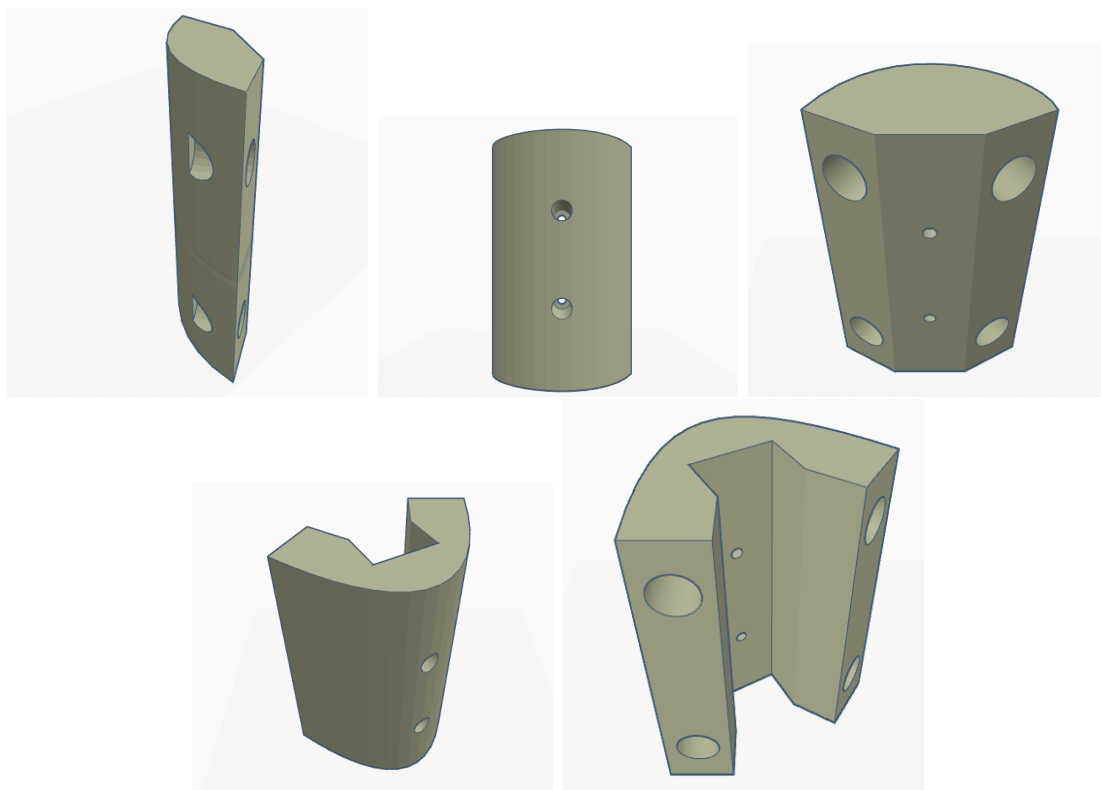


Figure 25: Iterations of the CAD for the 3D printed end caps

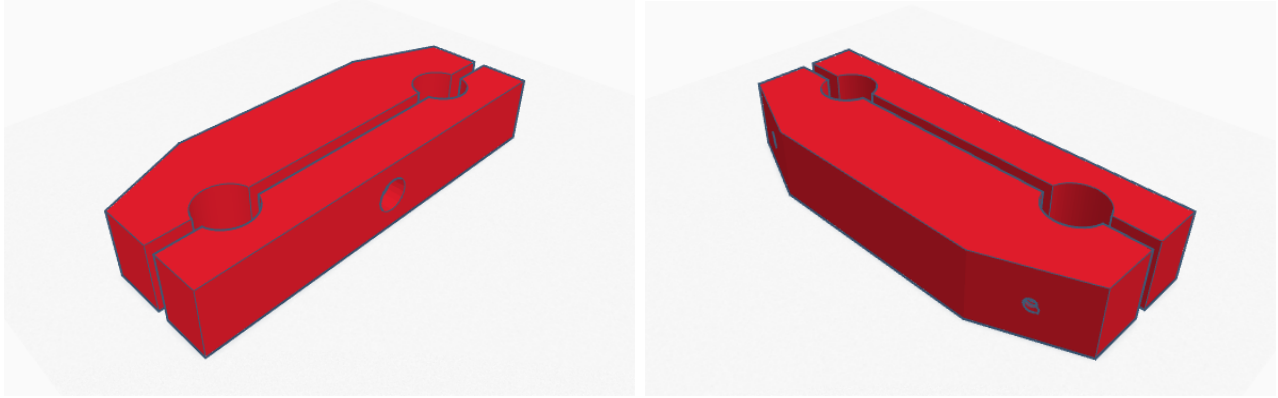


Figure 26: Calibration orb mounting bracket CAD iterations

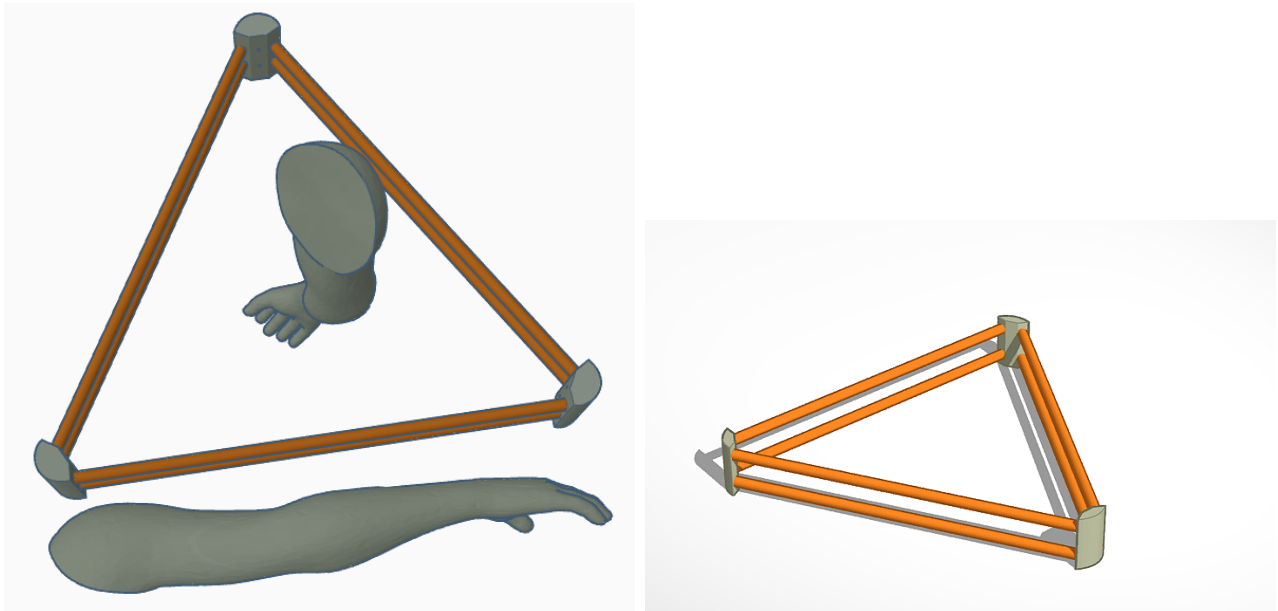


Figure 27: CAD for assembled VIRIS frame with arm length comparisons

## B Bill of Materials

Item	Item Cost	Quantity	Total Cost
Intel RealSense D435 Camera <sup>30</sup>	£135.71	3	£407.13
StarTech TB33A1C <sup>36</sup> with 65W DC Power Supply	£145.32	1	£145.32
Hollow Aluminium Tube ID: 12.6mm OD: 15.8mm	£1.57	6	£9.42
USB-C to USB-A 10Gbps Cable	£5	3	£15
Thunderbolt 3.0 to Thunderbolt 3.0 Cable	£80	1	£80
Brass Rod ø6mm	£6	1	£6
		<b>Total</b>	<b>£662.87</b>

## C Study Participant Information Document



Department of Bioengineering  
Imperial College London  
South Kensington Campus  
London, SW7 2AZ  
Tel: +44 (0)20 7594 0747

Investigators: Prof. James E. Moore Jr.  
Mr. Samuel Karet

### “Cyclic Vacuum Device for Modulating Lymphatic Pumping”

#### **Participant Information Sheet**

Professor James Moore Jr. and his research team would like to invite you to participate in a research study. Before you agree to participate, it is important for you to understand the motivation behind this research and what the study entails. This document provides detailed information about the research study and is yours to keep. Please take the time to read the following sections carefully before you decide whether or not you wish to take part. If there is anything that is not clear or if you would like more information, please do not hesitate to speak to the investigators.

#### **What is the purpose of the study?**

Lymphoedema is a disfiguring and incurable disease characterized by an accumulation of interstitial fluid in the face, arms, legs or abdominal walls due to a failure in the lymphatic system, which is in charge of transporting this fluid. Currently, the most common treatment consists of a combination of compressive bandages and massages aimed to reduce swelling by compressing the affected area. However, according to a computational model developed by Imperial College researchers, the flow of fluid in the lymphatic system increases when the pressure around the limb is reduced, not increased.

To confirm this theory, a medical device has been developed to apply alternating vacuum and compression to an arm. If we can measure and demonstrate a significant change in volume of the arm after using the device on the arm of a healthy volunteer, this will lead us to try the device on patients with lymphoedema. The quantitative results of this study will be critical in

# Imperial College London

determining if this technology is a viable complement and/or replacement for current treatments.

## **Why have I been chosen?**

We request your participation as a healthy adult with no pain or injury on the arm that will be tested. You do not suffer from any cardiovascular disease (especially arterial or cardiac insufficiency) or any other medical disorders that may worsen due to the application of vacuum and/or compression to a limb. Please note that if you are unable to speak or read English, or suffer from a psychiatric illness that affects your ability to give informed consent, you will be excluded from the study.

## **Do I have to take part?**

No, your decision to participate is entirely up to you. If you would like to take part, you will be asked to sign a consent form. Note that even after you have signed the consent form and agreed to join the study, you are free to withdraw from the study at any time. If you decide not to take part, or withdraw from the study, it will not affect any future interactions that you may have with Imperial College. The information collected up until that point will be retained and used in the study; however, no further data will be collected. Please inform any member of the research team straight away if you no longer wish to participate in the study.

## **What does participation in the study involve?**

Once you have decided to take part in this research, you will be asked to come to the South Kensington Campus of Imperial College London, SW7 2AZ, where our research team will discuss the study with you and answer any questions you may have. If you are still happy to take part, we will ask you to sign the consent form. During this visit, you will be asked to complete a short questionnaire. You will only be required to make one visit to the laboratory, lasting approximately 80 minutes.

We will ask you to provide us with some information regarding your age, gender, height, weight, and any history of cardiovascular and/or lymphatic disease (Appendix 5). Once completed, we will measure your arm's volume using three different techniques. The first is a water volumeter, where you will submerge your arm into a water tank and the displaced fluid will be measured. The second is a scanning modality that uses an infrared camera. The final technique uses small electrical signals to measure fluid in the arms. Afterwards, we will put you the medical device and the treatment will start. It will last up to 45 minutes, and during this time you will be asked to remain seated. Then, the device will be taken off and the volume of your arm will be measured again.

## **Imperial College London**

Finally, we will ask you to wait 15 more minutes so we can measure the volume one final time to document any other changes. Note that the contralateral arm will be measured at the same time points and these measurements will be used as control.

### **What are the side effects, and are there any risks in taking part?**

The pressure applied to your arm may cause some numbness or irritation. If you have any skin condition or small injury, please inform the researcher prior to the start of the test, as you may be unable to take part. If you notice any discomfort during or immediately following the study, please inform the researcher and a first aider will be called to assist you. If the irritation persists for more than 24 hours, please contact us and you may be advised to consult your local medical clinic. Remember that if you want to stop and/or withdraw, you can do so at any time.

### **What are the possible benefits of taking part?**

There are no direct personal benefits to you of taking part in this study. However, the information we collect from this research will help us demonstrate the effectiveness of a potentially revolutionary treatment for lymphoedema patients and to confirm the reliability of the computational model where the hypothesis of the treatment is based. In the long term, it will pave the way for the development of a medical device that uses this technique to help millions of people.

### **Will my taking part in this study be kept confidential?**

Any information you give us will be kept confidential. If the study is published in a book or scientific journal, no individual will be identified in any way. Your personal details will be stored on a protected computer belonging to Imperial College London.

### **What will happen to the results of the research study?**

The results of the study will be analysed by the research team and presented at scientific and clinical conferences and published in scientific journals. No individual subject will be identified in any report or presentation arising from the research. Note also that we are unable to provide you with your individual results. However, you can be provided with a summary report of our findings at the end of the study, upon your request.

### **Will I be paid for taking part in the study?**

You will not be paid for your participation in the study.

### **Who has reviewed the study?**

# Imperial College London

This study was reviewed by the Joint Research Compliance Office (JRCO).

## **What happens in case of withdrawal?**

As a participant, you will be informed of your right to leave the study at any time without giving any reason. To withdraw from the project, you must make it clear to the investigators. This can be done during or at the end of the research by any of these methods: using the contact email provided in this sheet, contacting one of the investigators using contact information provided in the university webpage, or speaking with one of the researchers directly. The data collected during the consent period will be stored and no further data of that subject will be recorded.

## **Contacts for further information:**

If you are considering taking part in the study and would like further information please contact [lymphatic\\_test@ic.ac.uk](mailto:lymphatic_test@ic.ac.uk).

## **LEGAL BASIS**

As a university we use personally-identifiable information to conduct research to improve health, care and services. As a publicly-funded organisation, we have to ensure that it is in the public interest when we use personally-identifiable information from people who have agreed to take part in research. This means that when you agree to take part in a research study, we will use your data in the ways needed to conduct and analyse the research study.

Health and care research should serve the public interest, which means that we have to demonstrate that our research serves the interests of society as a whole. We do this by following the UK Policy Framework for Health and Social Care Research.

## **INTERNATIONAL TRANSFERS**

There may be a requirement to transfer information to countries outside the European Economic Area (for example, to a research partner). Where this information contains your personal data, Imperial College London will ensure that it is transferred in accordance with data protection legislation. If the data is transferred to a country which is not subject to a European Commission (EC) adequacy decision in respect of its data protection standards, Imperial College London will enter into a data sharing agreement with the recipient organisation that incorporates EC approved standard contractual clauses that safeguard how your personal data is processed.

## **CONTACT US**

If you wish to raise a complaint on how we have handled your personal data or if you want to find out more about how we use your information, please contact Imperial College London's Data Protection Officer via email at [dpo@imperial.ac.uk](mailto:dpo@imperial.ac.uk), via telephone on 020 7594 3502 and



via post at Imperial College London, Data Protection Officer, Faculty Building Level 4, London SW7 2AZ.

If you are not satisfied with our response or believe we are processing your personal data in a way that is not lawful you can complain to the Information Commissioner's Office (ICO). The ICO does recommend that you seek to resolve matters with the data controller (us) first before involving the regulator.

### **Use of Research Data**

When you agree to take part in a research study, the information about your health and care may be provided to researchers running other research studies in this organisation and in other organisations. These organisations may be universities or companies involved in health and care research in this country or abroad. Your information will only be used by organisations and researchers to conduct research in accordance with the [UK Policy Framework for Health and Social Care Research](#).

This information will not identify you and will not be combined with other information in a way that could identify you. The information will only be used for the purpose of health and care research, and cannot be used to contact you or to affect your care. It will not be used to make decisions about future services available to you, such as insurance.

## D Study Consent Form



Department of Bioengineering  
Imperial College London  
South Kensington Campus  
London, SW7 2AZ  
Tel: +44 (0)20 7594 0747

Subject Identification Number for this trial: \_\_\_\_\_

### CONSENT FORM

#### Cyclic Vacuum Device for Modulating Lymphatic Pumping

Investigators: Professor James E. Moore Jr. and Mr. Samuel Karet.

Please initial  
the boxes

1. I confirm that I have read and understand the Participant Information Sheet dated 01/03/2019 for the above study and have had the opportunity to ask questions.
2. I understand that my participation is voluntary and that I am free to withdraw at any time without giving any reason, and without my legal rights being affected.
3. I agree to my anonymised data being stored on password protected Imperial College London computer systems.
4. I agree to take part in the above study.
5. I would like to be provided with a summary report of our findings at the end of the study, at my request.

---

Name of subject

---

Date

---

Signature

---

Name of person taking consent

---

Date

---

Signature

## E MATLAB Code

For all the code used for this project, visit the associated GitHub repository,  
<https://github.com/Motus-Lymph/VIRIS>  
Contact d.watson@imperial.ac.uk for access.

### E.1 Post Processing Testing

The code used to automate post-processing of all the scans taken during the study.

```
1
2
3
4 %>>> %% Load Non-VIRIS Measurements
5 StudyMeasurements;
6 %% Load all files from Study and assign their filenames to an indexed variable
7 ScanList = dir('C:/VIRIS/ScansStudy/');
8 cd 'C:/VIRIS/ScansStudy/'
9 %k =1 means left arm, k=2 means right arm
10 for i=1:11
11     for k =1:2
12         for j=1:4
13             if k==1
14                 FileID = [];
15                 FileID = strcat('*SubjectScan_',num2str(i),'_Stage',num2str(j),
16                               '_L_* .mat');
17                 FileName{i}{j}{k} = dir(FileID);
18             else
19                 FileID = [];
20                 FileID = strcat('*SubjectScan_',num2str(i),'_Stage',num2str(j),
21                               '_R_* .mat') ;
22                 FileName{i}{j}{k} = dir(FileID);
23             end
24         end
25     end
26 end
27 %% Run each file through post-processing
28 cd 'C:/VIRIS/'
29 for i=1:11
30     for k=1:2
31         for j=1:4
32             m = sprintf('%d%d%d',i,k,j)
33             if k==1
34                 try
35                     Subject{i}.left.Geometries{j} = ResultsPostFunction(FileName{i}
36                                         ){j}{k}.name,Subject{i}.left.tip2usp,Subject{i}.left.
37                                         tip2shoulder);
38                 catch
39                     warning(sprintf('Subject%d.L.Stage%d Threw a Volume
40                               Measurement Error',i,j))
41                 end
42             end
43         end
44     end
45 end
```

```
37     else
38         try
39             Subject{i}.right.Geometries{j} = ResultsPostFunction(FileName{i}
40                 }{j}{k}.name,Subject{i}.right.tip2usp,Subject{i}.right.
41                 tip2shoulder);
42             catch
43                 warning(sprintf('Subject%d.R.Stage%d Threw a Volume
44                     Measurement Error',i,j))
45             end
46         end
47     end
48 end
```